ChemComm

Regulable high-contrast mechanofluorochromic enhancement behaviour based on substituent effects

Journal:	*ChemComm*
Manuscript ID	CC-COM-01-2024-000476.R1
Article Type:	Communication

COMMUNICATION

Regulable high-contrast mechanofluorochromic enhancement behaviour based on substituent effects

Received 00th January 20xx,
Accepted 00th January 20xx

DOI: 10.1039/x0xx00000x

Guang Yang,‡[a] Wen-Xuan Zhao,‡[a] Jing-Yi Cao,[a] Zeng-Min Xue,[a] Hong-Tao Lin,[a] Shu-Hai Chen,*[a] Takehiko Yamato,*[b] Carl Redshaw[c] and Chuan-Zeng Wang*[a]

Herein, a facile strategy was established to build mechanoresponsive luminogens with high sensitivity to substituents and positional effects. Even in slightly different structures, distinct optical phenomena, including fluorescent efficiency and mechano-responsive properties were clearly present. Outstanding mechanical-induced emission enhancement (5–100 times) properties and reversibility by multiple cycles of grinding–fuming procedures makes for promising applications in pressure sensors and OLEDs.

The class of mechanofluorochromic (MFC) luminogenic materials has been and continues to be a research field of great interest and significance in terms of the design and synthesis of smart photoelectric materials.[1] Due to their ability to trigger fluorescent colour transient responses immediately after external mechanical stimulation, they are widely used in security encryption devices, anti-counterfeit ink materials, photosensitive sensors, organic light-emitting diodes (OLEDs), fluorescent probes.[2] Although mechanoresponsive molecules with tunable appearance colour or emission colour has enormously enriched the Mechanochromic luminogenic (MCL) materials and even smart material family, the rational tuning of the mechano-induced bathochromic/hypsochromic shift, emission enhancement, remains an outstanding challenge.[3]

Pyrene, as a classical chromophore, has received widespread attention due to its excellent blue emitting properties, high quantum yield, enhanced carrier mobility, and good thermal stability.[4] However, many pyrene-based luminophores suffer from the plaguing aggregation-caused quenching (ACQ) phenomenon due to excimeric/dimeric emission in the aggregated state.[5] Tremendous efforts have been made to improve pyrene luminophores over the past few years by employing some effective methods, such as introducing bulky substituents to inhibit the formation of dimers, constructing aggregation-induced emission luminogens (AIEgens) and smart MCL materials.[6] A diversity of promising strategies have been established to achieve functionalized pyrene derivatives with improved photoluminescence properties.

Normally, most AIE-active materials are susceptible to various mechanical stimuli responses.[7] Thus, the most efficient strategy to construct MFC luminogens comes down to the point of the design of pyrene-based AIEgens. An effective approach to obtain the above mentioned structures is to introduce typical AIE units at the pyrene core,[6] such as tetraphenylethylene (TPE),[8] hexaarylbenzene (HAB),[9] cyanoethylene unit, and so on.[7] Subsequently, non-typical pyrene-based AIEgens were prepared by employing the chalcone unit, Schiff base moieties, and excited-state intramolecular proton transfer (ESIPT) molecular systems. Meanwhile, novel mechanochromic luminescent materials formed by appending a pyrene moiety to benzophenone (**BP**) units were explored, and their attractive and interesting photophysical properties were mainly derived from the electron withdrawing ability of **BP** and the chromophore pyrene.[10]

Herein, we report mechano-responsive luminescence variations in D-A-D type architectures by combining electron-withdrawing benzophenone and electron-donating pyrene unit *via* a Suzuki coupling reaction (Scheme 1). The detailed synthesis and characterization of the four pyrene-based benzophenone derivatives is shown in Scheme S1-S4 and Fig. S1-S14 (ESI†). A set of regulable high-contrast mechanofluorochromic materials with excellent thermal stability and mechano-induced emission enhancement behaviour based on substituent and position-dependent effects were investigated.

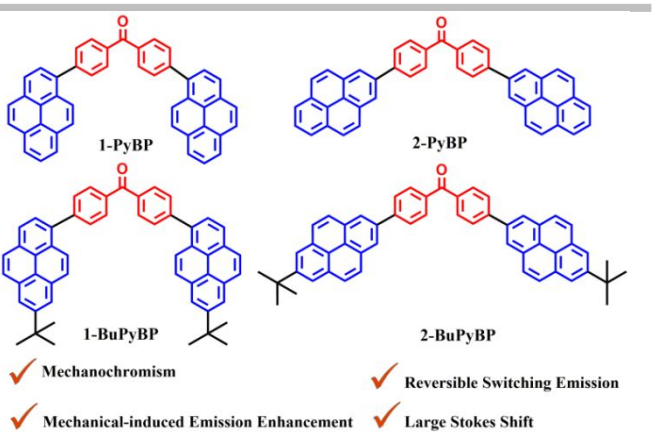

Scheme 1. Molecular structures of four luminogens.

[a] School of Chemistry and Chemical Engineering, Shandong University of Technology, Zibo 255049, P. R. China. Email: csh210302@163.com, czwang@sdut.edu.cn
[b] Department of Applied Chemistry, Faculty of Science and Engineering, Saga University Honjo-machi 1, Saga 840-8502 Japan. Email: yamatot@cc.saga-u.ac.jp
[c] Chemistry, School of Natural Sciences, The University of Hull, Cottingham Road, Hull, Yorkshire HU6 7RX, UK

† G Y and W.-X. Z. contributed equally to this work.

Electronic Supplementary Information (ESI) available: [details of any supplementary information available should be included here]. See DOI: 10.1039/x0xx00000x

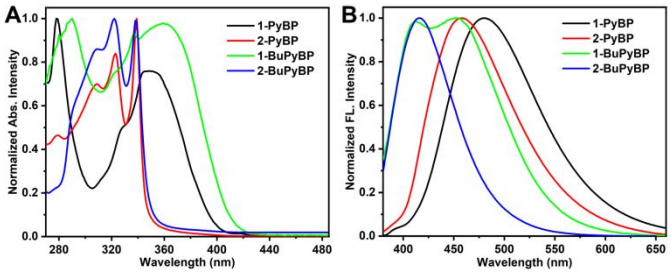

Fig. 1 Normalized absorption (A) and emission spectra (B) of the four luminogens in THF solution.

The photophysical properties of the four luminogens were studied in organic solutions and in the solid state; detailed parameters are recorded in Table S1. Two kinds of absorption spectra were observed in this system, obviously, the 1/2-substituted positions have an effect on their absorption behaviour (Fig. 1A and Fig. S15-S18, ESI†). Specifically, a wide absorption in the long-wavelength band and a narrow absorption in the short-wavelength band were present for 1-substituted structures, while the opposite phenomenon of absorption band width was observed for 2-substituted structures, which can be attributed to the position effect. Interestingly, the maximum absorption wavelengths displayed significant position-dependent effects, the maximum absorption wavelength centered at 278 nm and 349 nm, 290 nm, 359 nm for **1-PyBP** and **1-BuPyBP**, respectively, while 323 nm and 339 nm for **2-PyBP**, 322 nm and 338 nm for **2-BuPyBP** were recorded, which can be attributed to the variable charge transfer (CT) character based on the substituent and position-dependent effects.[11] Similarly, the synergistic effect of the substituent and its position plays a significant role in the emission behaviour in these systems in dilute organic solution and in the solid state. As shown in Fig. 1B, an obvious bathochromic shift was recorded with a maximum emission wavelength at 480 nm for **1-PyBP**, 412 nm and 451 nm for **1-BuPyBP** in dilute solution when the 1-positon was occupied by the **BP** unit, whilst a short emission wavelength was centered at 458 nm for **2-PyBP** and 416 nm for **2-BuPyBP**, which can be attributed to the controllable intramolecular charge transfer (ICT) emission state by employing the substituent and position-dependent effects.[12] Meanwhile, a dual emission similar as shoulder peak was observed for **1-BuPyBP**, which is mainly attribute to the solvent relaxation in the excited state based on butyl substituent effects. Moreover, the solvatochromic effects further interpreted the above emission behaviour (Fig. S19-S22, ESI†). As shown in Fig. S23, ESI†, the trend of bathochromic-shifts and sensitivity toward the solvent polarity of the four luminogens with the CIE 1931 chromaticity diagram are in line with the absorption spectra of solvatochromic effects, which is mainly attributed to different charge communication in the four molecular systemsbased on substituent and position-dependent effects, and a promising substituent and position-sensitive strategy was established for the design in pyrene-based luminogen systems.

Moreover, the extraordinary sensitivity to substituent and position effects further stimulated our interest to explore their photophysical properties in the solid state. As expected, these compounds also exhibited distinct emission properties and absolute fluorescence quantum yields (ϕ_{FL}). Specifically, as shown in Fig. 2A, the 1-substituted compounds **1-PyBP** and **1-BuPyBP** present long maximum emission wavelength at 511 nm and 500 nm, respectively. On the other hand, short emission wavelength centered at 469 nm for **2-PyBP** and 454 nm for **2-BuPyBP** was observed as 2-substituted derivatives, which can be attributed to the synergistic effect of ICT, molecular configurations and packing arrangement.[13] On the one hand, substituents play a significant different roles in interacting with the HOMO/LUMO orbitals of pyrene at the 1-position or 2-position, which results in a profound influence on the photophysical properties by regulating the ICT behaviour.[14] On the other hand, the bulky blocking *tert*-butyl group can affect the packing arrangement in the aggregate state, which also results in the transformation of the monomer emission and excimer emission due to the exciton coupling, π-π interactions, and dimer overlap between the adjacent molecules.[15] Thus, the above four luminogens present distinct emission properties resulting from the synergistic effect of the substituent and substituted position effects.

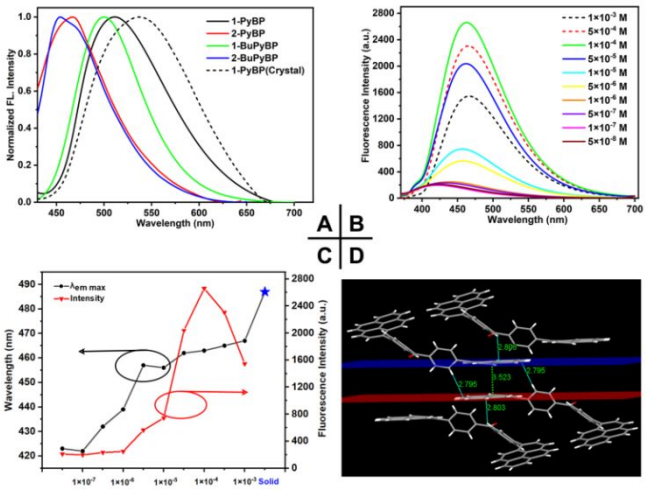

Fig. 2 (A) Normalized fluorescence emission spectra of four luminogens and crystal of **1-PyBP**; (B) Effect of concentration on the fluorescence emission spectra of **2-PyBP** recorded in THF at room temperature; (C) Plots of maximum emission wavelength (black circle) and emission intensity (red circle) of **2-PyBP** in different concentrations; (D) Intermolecular interactions in crystals of **1-PyBP**.

The value of ϕ_{FL} exhibited great variation from the dilute organic solution to the solid state and between each other. All compounds, except for **1-BuPyBP**, exhibit high quantum yields in solution than in the solid state, which can be attributed to the formation of dimer/excimer (π···π interactions) and through-space charge transfer (TSCT) in the aggregation state.[16] Because of the presence of the bulky *tert*-butyl group at the 7-position of the pyrene core, **1-BuPyBP** presents a high quantum yield (77.5%). Subsequently, the concentration effects were investigated in THF at room temperature. Taking **2-PyBP** as an example, Fig. 2B shows the fluorescence emission spectra at different concentrations. A trend in emission intensity of gradual enhancement from 5×10^{-8} M to 1×10^{-4} M and then decreased from 1×10^{-4} M to 1×10^{-3} M was observed upon increasing the concentration. As shown in Fig. 2C, a more intuitive presentation indicated that the maximum emission wavelength with increasing concentration displayed a persistent red-shift towards the maximum emission wavelength of the solid powder, and understandably, the change of dominance from the

monomeric emission to the dimeric/excimeric emission is certainly happening. The other three compounds also present a similar trend and emission properties (Fig. S24-S26, ESI†). Fortunately, crystals of **1-PyBP** suitable for single crystal X-ray diffraction (XRD) (Fig. 2D) were obtained; detailed structural information is summarized in Table S1, ESI†. Obvious face-to-face π···π stacking interactions (3.523 Å) and end-to-face C–H···π hydrogen bonds (2.795–2.803 Å) are found in packing behaviour. The weaker luminescence in the solid state (ϕ_{FL} = 5%) than in solution (ϕ_{FL} = 17.1%) may be ascribed to the formation of π-aggregates /excimers between the neighbouring molecules. The emission spectrum of **1-PyBP** in the crystalline state was then measured (dashed line in Fig. 2A) and, as expected, a more pronounced red-shift (from 511 nm to 537 nm) and lower quantum yield (ϕ_{FL} = 1.7%) were recorded compared to the solid state. This is mainly attributed to the synergistic influence of the inter/intramolecular charge transfer state and formation of pyrene dimeric/excimeric emission.[17] As shown in Fig. S27, the decay curves were fitted as a double exponential decay, showing the fluorescence lifetime of τ = 1.06 ns for **1-PyBP**, 1.69 ns for **2-PyBP**, 0.99 ns for **1-BuPyBP**, and 3.88 ns for **2-BuPyBP**, respectively. The τ of these compounds was increased by about 2–5 times in the solid or crystalline states, which may be attributed to the weakened molecular motion in the aggregated state.[18] The radiative decay rate constant k_r and the non-radiative decay rate constant k_{nr} were recorded in Table S2, which are consistent with their emission behaviour.

The investigation of their mechanical stimuli-responsive properties was performed by a grinding treatment, and the difference in the mechano-fluorochromic property was further markedly magnified. All compounds, except for **1-BuPyBP**, present obvious mechanochromism (MC) properties with the mechanical force as the excitation source. Moreover, an interesting phenomenon of fluorescent colour along with the mechanically-induced emission enhancement (MIEE) was observed, and the dramatic enhancement of the fluorescence quantum yield up to 5–100 times is rare in other reported work on pyrene-based MFC luminogens or even all MFC luminogenic materials.[19]

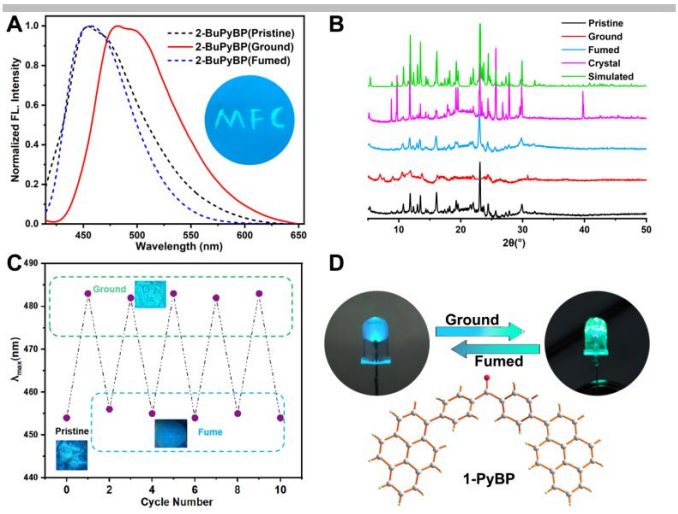

Fig. 3 (A) The normalized PL and MCL spectra of **2-BuPyBP**; (B) PXRD patterns of as-prepared powder of **1-PyBP** and their samples after grinding, fuming and simulated data by crystal; (C) Reversible switching emission of pristine powder of **2-BuPyBP** by repeating grinding–fuming cycles (Insets in C: photograph changes of **2-BuPyBP** in grinding–fuming cycles); (D) The pristine (left) and ground (right) powder of **1-PyBP** was coated on the UV-LED lamp (the LED lamp with an excitation wavelength of 365 nm was selected), bluish-green and green luminescence were observed after power on, respectively.

As shown in Fig. 3 and Figs. S28-S30 in ESI†, the mechano-fluorochromic properties were systematic studied including fatigue tests and application in LED display technology. Different bathochromic shifts with 7 nm for **1-PyBP**, 30 nm for **2-PyBP**, 29 nm for **2-BuPyBP** were observed upon grinding. Taking **2-BuPyBP** as an example, it exhibited a sky-blue colour ($\lambda_{max\ em}$ = 454 nm), which upon grinding changed to a blue-green colour ($\lambda_{max\ em}$ = 483 nm) under 365 nm UV light (Fig. 3A inset). Interestingly, the fluorescence quantum yield is greatly improved from 0.5% for the pristine powder to 49.2% for the ground sample, which is an unimaginable change for a non-AIE active luminogen, which is mainly attributed to the dissipation of π-aggregates by significant interlayer slipping. After all, more than a tenfold increase in ϕ_{FL} compare to in dilute solution (ϕ_{FL} = 3.6%) makes this a competitive pyrene-based luminogenic material. Powder XRD (PXRD) was performed to elucidate the mechanism of mechanochromism (to see Fig. 3B and Fig. S31 in ESI†), and three materials exhibited significant transformation from the crystalline phase to an amorphous state with the disappearing of diffraction peaks after grinding. More convincingly, as shown in Fig. 3B, the systematic and comprehensive PXRD analysis, including single crystal structure, as-prepared pristine powder, and the sample after grinding, indicated that distinct intramolecular interactions and arrangements exist in the different systems. Obvious π···π interactions were observed in the single crystal structure, which result in the red-shifted emission and low ϕ_{FL} value compared to the pristine powder. The intense and sharp diffraction peaks for the pristine powder are different from the single crystal structure, which indicated that it is in a crystalline state with a slight slip of the adjacent pyrene core. A significant inter-layer slippage further occurred during the grinding process, and the fluorescent efficiency is greatly improved based on the weakening of the excimer emission.[20] In view of these explorations, the compound **1-BuPyBP** without mechanical response may be ascribed to the dense molecular arrangement and intermolecular interactions. Moreover, almost identical PXRD results (Fig. S32 in ESI†) and slightly raised ϕ_{FL} value after grinding fully verified this hypothesis. Then other three set of PXRD results all present obvious change with mechanical grinding.

Fatigue tests were carried out by multiple cycles of grinding–fuming procedures (Fig. 3C and Fig. S33 in ESI†). Efficient reversibility is demonstrated by repeated grinding and fumigation with DCM. Meanwhile, similar diffraction peaks in the PXRD were observed by solvent fuming compared to the pristine sample which can be attributed to the excellent reversibility of the crystalline-to-amorphous conversion. In view of the above excellent material performance, a light-emitting diode (LED) was fabricated. Samples before and after grinding are coated onto the surface of a commercially available 365 nm UV LED, as shown in Fig. 3D. When the LED is energized, the LED coated with pristine sample emits a faint bluish-green light, while the LED coated with ground sample emitted a strong green light. The outstanding reversibility and

fluorescent efficiency bestow a promising application potential in the area of organic LEDs (OLEDs).

In order to optimize the molecular geometries and to gain insight into the electronic transition mechanism at the molecular level, density-functional theory (DFT) calculations were performed using the B3LYP/6-31G (d, p) motif implemented in the Gaussian 09W program.[21] As shown in Fig. S34, the spatial distributions of the electron densities of the four structures in the highest occupied molecular orbital (HOMO) and the lowest unoccupied molecular orbital (LUMO) exhibited excellent delocalization performance. The HOMOs of these four compounds are predominantly distributed over the pyrene core of the distorted portions. For **1-PyBP** and **1-BuPyBP,** LUMO energy level electron densities are distributed over the whole molecule, for the electron density of **2-PyBP**, **2-BuPyBP**, LUMO energy level is mainly concentrated at the benzophenone unit and slightly localized towards the pyrene core at both terminals, which can be ascribed to the larger conjugation structure and more delocalized LUMO for the 1-substituated derivative. A more obvious separation of the HOMO and LUMO distribution for the 2-substituted derivatives was observed, which is mainly attributed to the weaker interaction between the substituents at the 2,7-positions and the HOMO/LUMO orbitals of pyrene as they lie on the nodal plane.[11, 22] As expected, the two substituent and position-dependent different sets of energy gaps (ΔE_g) further confirmed our previous interpretation of the ICT behaviour in this MFC luminogen system.

In summary, four simple but interesting MFC luminogens were synthesized and characterized. A design strategy of mechanical stimuli-responsive materials with high sensitivity to substituents and position effects was established. Moreover, most of these compounds exhibited outstanding mechanically-induced emission enhancement (MIEE), with an improvement in fluorescence quantum yields of more than 100 times. It is also noteworthy that the excellent reversibility for mechanical stimulation and fluorescent efficiency, especially for the ground sample, can be utilized for LEDs materials in the field of display technology. Further explorations aimed at developing advanced sensor systems with distinct emission-colour switching for detection of mechanical stimuli are ongoing in our group.

This work was performed under the Cooperative Research Program of "Network Joint Research Center for Materials and Devices (Institute for Materials Chemistry and Engineering, Kyushu University)". We would like to thank the Natural Science Foundation of Shandong Province (Grant No. ZR2019BB067), this research used resources of the Advanced Light Source, which is a DOE Offce of Science User Facility under contract no. DE-AC02-05CH11231. CR thanks the University of Hull for support.

Conflicts of interest

There are no conflicts to declare.

Notes and references

1 (a) J. Zhang, B. Z. He, Y. B. Hu, P. Alam, H. K. Zhang, J. W. Y. Lam and B.-Z. Tang, *Adv. Mater.*, 2021, **33**, 2008071; (b) Z. G. Chi, X. Q. Zhang, B. J. Xu, X. Zhou, C. P. Ma, Y. Zhang, S. W. Liu and J. R. Xu, *Chem. Soc. Rev.*, 2012, **41**, 3878−3896; (c) J. Q. Gu, Z. Li and Q. Q. Li, *Coord. Chem. Rev.*, 2023, **475**, 214872.

2 (a) L. Bai, P. Bose, Q. Gao, Y. Li, R. Ganguly and Y. Zhao, *J. Am. Chem. Soc.*, 2017, **139**, 436–441; (b) S. Q. Ma, S. J. Du, G. C. Pan, S. T. Dai, B. Xu and W. J. Tian, *Aggregate*, 2021, **2**, e96.

3 (a) J. Wang, B. Yue, X. Jia, R. Cao, X. Niu, H. Zhao, J. Li and L. Zhu, *Chem. Commun.*, 2022, **58**, 3517–3520; (b) R. Yoshida, T. Tachikawa and S. Ito, *Chem. Commun.*, 2022, **58**, 6781–6784.

4 (a) X. Feng, X. H. Wang, C. Redshaw and B. Z. Tang, *Chem. Soc. Rev.*, 2023, **52**, 6715−6753; (b) T. M. Figueira-Duarte and K. Mullen, *Chem. Rev.*, 2011, **111**, 7260–7314.

5 Z. Zhang, B. Xu, J. Su, L. Shen, Y. Xie and H. Tian, *Angew. Chem., Int. Ed.,* 2011, **50**, 11654–11657.

6 (a) M. M. Islam, Z. Hu, Q. S. Wang, C. Redshaw and X. Feng, *Mater. Chem. Front.*, 2019, **3**, 762–781; (b) V. A. Dini, D. Genovese, C. Micheletti, N. Zaccheroni, A. Pucci and C. Gualandi, *Aggregate*, 2023, **4**, e373.

7 J. Zhao, Z. Chi, Y. Zhang, Z. Mao, Z. Yang, E. Ubbab and Z. Chi, *J. Mater. Chem. C*, 2018, **6**, 6327–6353.

8 X. Feng, C. Qi, H.-T. Feng, Z. Zhao, H. H. Y. Sung, I. D. Williams, R. T. K. Kwok, J. W. Y. Lam, A. Qin and B. Z. Tang, *Chem. Sci.*, 2018, **9**, 5679–5687.

9 C. Z. Wang, Y. Noda, C. Wu, X. Feng, P. Venkatesan, H. Cong, M. R. J. Elsegood, T. G. Warwick, S. J. Teat, C. Redshaw and T. Yamato. *Asian J. Org. Chem.*, 2018, **7**, 444–450.

10 Y. Xiong, J. Huang, Y. Liu, B. Xiao, B. Xu, Z. Zhao and B. Z. Tang, *J. Mater. Chem. C*, 2020, **8**, 2460–2466.

11 J. Merz, M. Dietz, Y. Vonhausen, F. Wöber, A. Friedrich, D. Sieh, I. Krummenacher, H. Braunschweig, M. Moos, M. Holzapfel, C. Lambert and T. B. Marder, *Chem. Eur. J.*, 2020, **26**, 438–453.

12 Z. D. Yu, X. X. Dong, J. Y. Cao, W. X. Zhao, G. H. Bi, C. Z. Wang, T. Zhang, S. Rahman, P. E. Georghiou, J. B. Lin and T. Yamato, *J. Mater. Chem. C*, 2022, **10**, 9310–9318.

13 G. Yang, K. Y. Liu, J. Y. Cao, J. Y. Yu, D. L. Sun, C. Z. Wang, W. X. Zhao, M. R. J. Elsegood, S. J. Teat, C. C. Zhu and T. Yamato, *Spectrochim. Acta - a: Mol. Biomol. Spectrosc.*, 2024, **305**, 123529.

14 (a) A. G. Crawford, A. D. Dwyer, Z. Liu, A. Steffen, A. Beeby, L.-O. P,lsson, D. J. Tozer and T. B. Marder, *J. Am. Chem. Soc.*, 2011, **133**, 13349–13362; (b) L. Ji, R. M. Edkins, A. Lorbach, I. Krummenacher, C. Bruckner, A. Eichhorn, H. Braunschweig, B. Engels, P. J. Low and T. B. Marder, *J. Am. Chem. Soc.*, 2015, **137**, 6750–6753.

15 H. C. Liu, L. Yao, B. Li, X.-K. Chen, Y. Gao, S.-T. Zhang, W.-J. Li, P. Lu, B. Yang and Y.-G. Ma, *Chem. Commun.*, 2016, **52**, 7356–7359.

16 C. Z. Wang, Z. D. Yu, W. X. Zhao, K. Yang, Y. Noda, Y. Zhao, X. Feng, M. R. J. Elsegood, S. J. Teat, C. Redshaw and T. Yamato, *Dyes Pigm.*, 2021, **192**, 109452.

17 J. Y. Cao, G. Yang, Z. M. Xue, W. X. Zhao, S. H. Chen, H. T. Lin, T. Yamato, C. Redshaw, D. Y. Gu, C. Z. Wang, *Dyes Pigm.*, 2023, **220**, 111758.

18 (a) X. Y. Song, H. X. Guo, S. N. Yu, L. Huang, C. Redshaw, Q. L. Zhang, R. Q. Ye, X. Feng, *Dyes Pigm.*, 2023, **210**, 111036; (b) X. Y. Wang, J. Y. Gong, H. Zou, S. H. Liu and J. Zhang, *Aggregate*, 2023, **4**, e252.

19 (a) P. Wen, Z. X. Gao, R. Zhang, A. R. Li, F. Zhang, J. Li, J. J. Xie, Y. Z. Wu, M. Wu and K. P. Guo, *J. Mater. Chem. C*, 2017, **5**, 6136–6143; (b) Y. Y. Zhang, T. Zhang, X. C. Wang, L. Kong and J. X. Yang, *Dyes Pigm.*, 2021, **188**, 109230.

20 T. Zhang, S. Chu, L. Lin, C.-Z. Wang, G. Gong, X. Song, J. Fan and S. Zhuo, *Chem. Phys. Lett.*, 2019, **734**, 136726.

21 S. Grimme, J. Antony, S. Ehrlich and H. Krieg, *J. Chem. Phys.*, 2010, **132**, 154104.

22 D. N. Coventry, A. S. Batsanov, A. E. Goeta, J. A. K. Howard, T. B. Marder and R. N. Perutz, *Chem. Commun.*, 2005, 2172–2174.

